

---

# MSA-LM: Integrating DNA-level Inductive Biases into DNA Language Models

---

Anonymous Author(s)

Affiliation

Address

email

## Abstract

1 Recent advances in DNA language modeling have been limited by computational  
2 constraints and the ability to capture long-range dependencies within genomic  
3 data effectively. While effective, traditional transformer-based models suffer from  
4 quadratic complexity and limited context windows, making them unsuitable for  
5 large-scale DNA modeling. In contrast, subquadratic models, while efficient, often  
6 lack bidirectionality and struggle with training scalability. We introduce MSA-  
7 LM, an inductive-bias-aware subquadratic DNA Multiple Sequence Alignment  
8 (MSA) model that addresses these limitations. MSA-LM integrates a bidirectional  
9 Mamba model for sequence mixing, providing transformer-like expressibility with-  
10 out the associated quadratic complexity. By utilizing a sparse attention mechanism,  
11 MSA-LM selectively processes the main DNA sequence while incorporating evolu-  
12 tionary information from MSA data, significantly reducing computational overhead.  
13 Our results demonstrate that MSA-LM achieves state-of-the-art performance on  
14 long-context variant effect prediction tasks and Genomic Benchmarks, particu-  
15 larly excelling in regulatory sequence analysis. The proposed model not only  
16 surpasses existing transformer-based and subquadratic approaches in efficiency but  
17 also maintains high accuracy across diverse genomic tasks, marking a significant  
18 improvement in DNA language modeling capabilities.

## 19 1 Introduction

20 Advances in model sizes and architectures have brought about a revolution in sequence modeling  
21 capabilities. The introduction of recurrence [26], attention [1], and memory [24] have led to many  
22 performance improvements. The transformer model [44], commonly used in large language models  
23 (LLMs) [6], applies self-attention and implicit memory [14] to sequence modeling.

24 Transformers have shown impressive generalization capabilities in natural language processing,  
25 prompting researchers to extend the models' abilities to sequences beyond language. Transformers  
26 have been applied to protein sequences [30] and genomics data [39]. Recently, they have been used  
27 in DNA modeling [10]. However, The human genome consists of 3 billion base pairs, with gene sizes  
28 ranging from 10 thousand to 2 million base pairs [32]. These large DNA sequences are expensive  
29 to analyze using a transformer due to the quadratic nature of self-attention [27] and the model's  
30 instability across extended context windows [31].

31 Subquadratic models ([38], [19], [16]) have been explored as alternate method to transformers for  
32 DNA modeling. They have shown high performance on Genomic Benchmarks tasks [41] and have  
33 context lengths ranging up to 128k base pairs [36].

34 Recent DNA language modeling methods have added information augmentations [2] or improved  
35 tokenizers/information aggregation to the original DNA sequence [40]. One of the most common

36 DNA augmentations is multiple sequence alignment (MSA) data. This information provides key  
 37 evolutionary relationship information relative to each base pair. Transformer-based methods for  
 38 DNA MSA processing have shown state-of-the-art performance in tasks with a basis in evolutionary  
 39 mutations (variant effect prediction) [3]. However, these models leverage quadratic sequence-wise  
 40 attention and axial attention-based methods, which do not scale well to long sequences. Because of  
 41 this, transformer-based DNA MSA models have only been trained at short context lengths<sup>1</sup>.

42 Subquadratic MSA models have been proposed as alternatives to transformer-based approaches  
 43 [43]. However, these models lack bidirectionality, hindering modeling accuracy greatly. In addition,  
 44 subquadratic MSA models are difficult to train at scale due to running subquadratic sequence mixers  
 45 on all auxiliary sequences in addition to the main sequence in an MSA. Batch size scaling is difficult  
 46 in these settings, leading to inefficient training and inference.

47 To correct the shortcomings of subquadratic DNA MSA models, we propose MSA-LM, an inductive-  
 48 bias-aware subquadratic DNA MSA model. This model leverages a bidirectional Mamba model as  
 49 a sequence mixer [25], which provides similar expressibility to full self-attention in transformers  
 50 without quadratic complexity. In addition, MSA-LM only runs the Mamba operation on the main  
 51 sequence, using sparse attention computations to integrate MSA data into one main sequence  
 52 representation [8]. Through this, we leverage MSA data as auxiliary information relative to the main  
 53 sequence and fix problems in the expressibility of previous subquadratic MSA models. Evaluations  
 54 of MSA-LM show state-of-the-art (SOTA) performance in 3 Genomic Benchmarks tasks<sup>2</sup> (see Table  
 55 6.2) and shows similar performance to SOTA models in long-context variant effect prediction (see  
 56 Table 6.1).

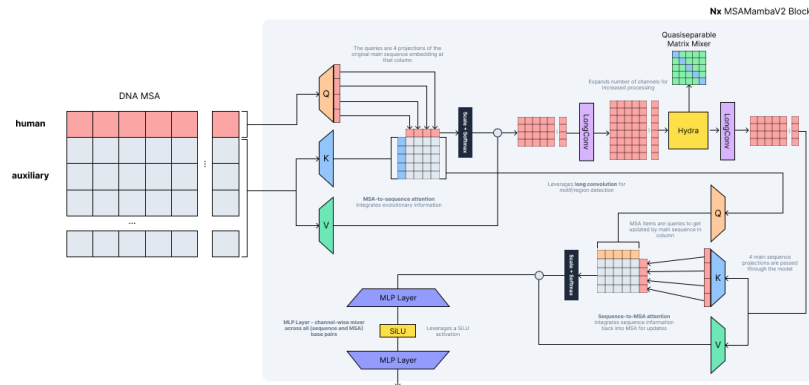


Figure 1: A diagram of the MSA-LM architecture. The architecture consists of multiple MSA-LM blocks, each of which contains a bidirectional mamba (quasiseparable matrix mixer) wrapped by long convolutions. It also includes an MSA to sequence mixer and a sequence to MSA mixer to integrate evolutionary information across the MSA.

## 57 2 Background

58 Deoxyribonucleic acid is a polymer made up of 4 base nucleotides (adenine, cytosine, guanine,  
 59 and thymine). The polymer forms a double helix structure from two complementary strands. DNA  
 60 contains regions known as genes, which can code for different proteins to cause cellular change.  
 61 Genes also consist of control sequences. These include enhancers, which can increase the DNA  
 62 transcription of a specific gene into a protein; promoters, which allow the initiation of transcription;  
 63 and silencers, which prevent transcription from occurring. [5]

64 DNA sequences contain introns and exons. Exons contain DNA information used to form the final  
 65 protein, while introns are non-coding regions that can be spliced out in different combinations to

<sup>1</sup>GPN-MSA, a prominent DNA MSA transformer model, trains on sequence lengths of 128, which cannot capture global relationships inherent in genomic data

<sup>2</sup>excluding dummy and demo datasets

66 create varying gene outputs. Genes can vary in length from thousands to millions of base pairs,  
 67 increasing the need for models with a large and effective context window.

68 **DNA MSAs** DNA Multiple Sequence Alignments (MSAs) are combinations of DNA sequences  
 69 across different species. These sequences are aligned such that base pairs that evolve similarly are  
 70 in the same column across genomes. Aligned columns in the MSA provide crucial evolutionary  
 71 information between species. A DNA sequence for a species can be considered as a function of a  
 72 different species' genome. This function consists of multiple mutations, such as insertions, deletions,  
 73 and replacements. By aligning these sequences using MSA creation algorithms, models can implicitly  
 74 extract conservation, coevolution, and homology information. DNA MSAs are also used to find  
 75 motifs (short, repetitive sequences across genes). Implicit detection of these motifs in AI models can  
 76 provide enhanced information for genome analysis. [42]

## 77 2.1 Transformer Models

78 Initial work in DNA language models involved leveraging the transformer architecture [44]. The  
 79 transformer consists of multiple blocks [9], each containing a self-attention and MLP block. The  
 80 self-attention block (see Eq. 1) functions as a fully connected sequence mixer, comparing all tokens to  
 81 each other without any causal or window-based restrictions<sup>3</sup>. The comparison operation is computed  
 82 using a dot product between two input space projections ( $Q, K$ ). This dot product is passed through  
 83 a row softmax and scaling operation before being multiplied by a value ( $V$ ) projection. This acts as a  
 84 weighted importance operation to emphasize important relationships while diminishing unimportant  
 85 ones.

$$O = \mathbf{softmax}\left(\frac{QK^T}{d_{attn}}\right)V \quad (1)$$

86 The MLP block acts as a channel-wise mixer, increasing the size of the model dimension from  $d_{model}$   
 87 to  $d_{ff}$  and decreasing back down to the model dimension. This upscaling and downscaling projection  
 88 allows for an integration with implicit memory that the transformer gains within its expanded MLP  
 89 weights while training. Between both operations, a residual connection [23] and normalization [45]  
 90 operation are included to prevent vanishing/exploding gradient problems during the backpropagation  
 91 process. [15]

92 Transformer models that have been applied to DNA-MSA modeling show high accuracy in evolution-  
 93 based modeling tasks. However, they have small context windows. This prevents transformers from  
 94 attending to long-context relationships between regions, motifs, and other areas across genes.

## 95 2.2 Subquadratic Models

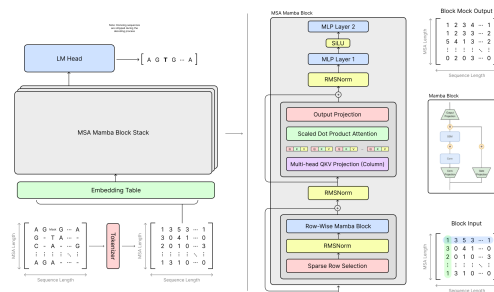


Figure 2: A diagram of the MSAMamba architecture, which leverages a selective-scan operation in the sequence dimension and a global-positioned attention process in the vertical dimension. [43]

96 Subquadratic models have initially been proposed as methods to decrease the expensive quadratic  
 97 complexity of transformers in language modeling. However, they have also been applied to DNA  
 98 modeling [19]. Some subquadratic models leverage long convolutions, which can be optimized to be

<sup>3</sup>Excluding masked tokens in the masked language modeling setting

99 computed in linear time [38]. These long convolutions can extract motif and region information, but  
 100 they lack expressibility with few channels. In addition, long convolutions cannot attend to global  
 101 relationships between regions due to the restrictivity of the kernel size and lack of state tracking  
 102 across long contexts [33].

103 State-space model methods [21] have been proposed to fix the shortcomings of long convolution-  
 104 based models. The original SSM formulation consists of four matrices that act as gates across a  
 105 continuous data stream.

$$106 \quad h_{t+1} = Ah_t + Bx_{t+1} \quad (2)$$

$$106 \quad y_{t+1} = Ch_{t+1} + Dx_{t+1} \quad (3)$$

107 In the discrete-time formulation, these matrices are discretized<sup>4</sup> [37] with a  $\Delta$  value representing a  
 108 step size across a continuous sequence.

$$\bar{A} = \exp(\Delta A) \quad (4)$$

$$\bar{B} = (\Delta A)^{-1}(\exp(\Delta A) - I)\Delta B \quad (5)$$

109 The original SSM formulation is linear time-invariant, allowing it to be computed as an efficient  
 110 1-dimensional convolution over a sequence. However, the Mamba SSM variant [19] makes the B, C,  
 111 and D matrices input-dependent, allowing more adaptability using gating (The A matrix is determined  
 112 using the HiPPO matrix formulation for long context data storage [20]). Although this model is no  
 113 longer time-invariant, it does not use activation functions, allowing the model to be computed in an  
 114  $O(N)$  associative scan [4] using a parallelized, hardware-aware kernel [11].

115 The original Mamba formulation was tested on Genomic Benchmarks tasks [18] and had shown  
 116 state-of-the-art performance on long-context tasks. However, it shows lower performance in shorter  
 117 contexts, while transformers excel.

118 MSAMamba has been proposed as an alternative subquadratic DNA MSA model that leverages  
 119 Mamba as the main sequence mixer [43]. While it shows improved performance compared to  
 120 transformer-based models in long-context variant effect prediction tasks and Genomic Benchmarks  
 121 tasks, it lacks training efficiency. MSAMamba runs a selective scan operation on all rows of the  
 122 MSA, which can prevent batch size scaling during training<sup>5</sup>.

## 123 3 Methods

124 We propose MSA-LM, a DNA MSA language model that improves the efficiency of previous methods  
 125 by running a bidirectional selective scan operation on only one main sequence. MSA information is  
 126 integrated into the main sequence using sparse attention across MSA data. In this section, we provide  
 127 an overview of the components and structure of MSAMamba.

### 128 3.1 MSA Attention

129 The MSA-LM block architecture consists of two MSA-length attention processes that integrate  
 130 MSA-level (column) and sequence-level (row) information. The first process is MSA-to-sequence  
 131 attention, which alters the full column-wise self-attention process to attend only to the first sequence’s  
 132 base pairs as a query. This integrates MSA information into the main sequence while preventing  
 133 inter-MSA attention<sup>6</sup>. In addition, this computation decreases the computational complexity of the  
 134 MSA attention process from quadratic to linear<sup>7</sup>, preserving the subquadratic nature of the model in  
 135 both the sequence and MSA dimensions.

<sup>4</sup>Recent work has shown that using the fixed HiPPO matrix and discretization cannot perform well in state-tracking tasks [33]. We acknowledge this approach, but we use the original Mamba implementation due to its memory-efficient selective scan kernel

<sup>5</sup>MSAMamba was trained on a physical batch size of 2 1024 base-pair sequences on a NVIDIA P100 GPU

<sup>6</sup>mixing of inter-MSA information is unnecessary, as only evolutionary information relative to the main sequence (human genome) is required

<sup>7</sup>with reference to MSA Length

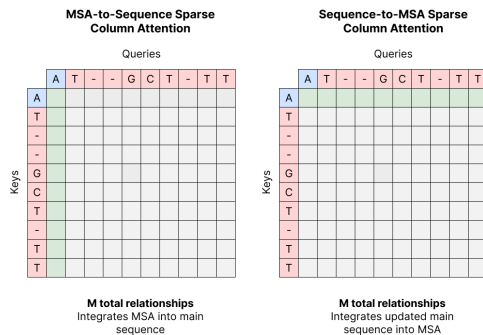


Figure 3: A diagram of the attention processes at the start and end of each MSA block. The MSA-to-sequence attention block acts as an integration of evolutionary information into the sequence, while the sequence-to-MSA attention process integrates sequence information into the MSA.

136 The second attention process is a sequence-to-MSA block, which integrates information present in  
 137 the main sequence with MSA information across an MSA column. Similar to the first attention block,  
 138 Inter-MSA relations are ignored for computational complexity benefits. With this formulation, other  
 139 parts of the algorithm only have to process the top sequence, since MSA information is implicitly  
 140 integrated and updated through these sparse attention processes.<sup>8</sup>

141 Each attention process consists of multiple sequence heads. This allows for multiple channels of  
 142 information to be integrated into the main sequence position in a column. This is integrated into the  
 143 channel formulation of the following convolution blocks.

### 144 3.2 Hydra + Convolution Block

145 The MSA-to-sequence block integrates MSA information into the target sequence. The auxiliary  
 146 MSA tensor is saved for the later sequence-to-MSA block but is not used in the Hydra and convolution  
 147 block computation<sup>9</sup>. There are  $n_{channels}$  number of channels in the output, based on the number of  
 148 query heads leveraged in the sequence-to-MSA attention block. These channels are then expanded  
 149 to  $expand \cdot n_{channels}$  by a long convolution block [17], which functions as a motif/region extractor  
 150 [35]. All channels of the main sequence are then passed to a bidirectional Mamba formulation [25].  
 151 The output of the Mamba algorithm is passed through another long convolution, which decreases  
 152 the number of channels back to  $n_{channels}$ . The output is passed to the sequence-to-MSA block to  
 153 integrate sequence information back into the MSA augmented information tensor.

154 Both long convolution blocks are implemented with a fast Fourier transform algorithm<sup>10</sup> [7]. The first  
 155 convolution operation expands the number of sequence channels. This expansion is done to increase  
 156 the number of computation heads in the bidirectional Mamba model to learn a robust representation  
 157 of the data. The second convolution decreases the number of channels.<sup>11</sup>

158 The output of the first convolution is passed as a multi-headed tensor to the bidirectional Mamba model.  
 159 We leverage the Hydra model, which uses a quasiseparable matrix mixer [25], to implement the  
 160 bidirectional mamba model<sup>12</sup>. Previous formulations use two Mamba models and add corresponding  
 161 outputs. However, the quasiseparable matrix formulation allows for higher training and inference  
 162 efficiency using two semiseparable matrix formulations [12].

<sup>8</sup>Both MSA attention processes leverage absolute position embeddings, which allows the model to identify each MSA species individually

<sup>9</sup>This is done to decrease the computational requirements of the main sequence mixer by integrating all information into one sequence

<sup>10</sup>FFT-based convolutions have shown higher performance at large kernel sizes

<sup>11</sup>For all models, we leverage an expansion factor of 2 and 4 main channels of computation. Scaling these factors can improve the representation capability of the model to handle longer contexts and more nuanced relationships.

<sup>12</sup>This model was chosen over other bidirectional Mamba formulations [41] due to increased computational efficiency

---

**Algorithm 1** MSA-LM Masked Language Modeling

---

**Input:** MSA  $x : (B, M, L, D)$ ,  $M_{row} : (B, M)$ ,  $y_t : (B, L, D)$ , lr,  $\theta$  (Model Params)

**Output:**  $y : (B, L, D)$

$h_0 = \text{mask}(x, p=0.15)$

**for**  $i = 1$  **to**  $n_{layers}$  **do**

$h_{sparse} = h_i[M_{row}]$

$O_{mamba} = \text{scatter}(\text{Mamba}(x_{sparse}), M_{row}) + h_i$

$O_{att} = \text{SelfAttention}(O_{mamba}) + O_{mamba}$

$h_{i+1} = \text{MLP}(O_{att})$

**end for**

loss = CrossEntropy( $h_{n_{layers}-1}[h_0 = \text{MASK}]$ ,  $y_t$ )

$\theta \leftarrow \text{AdamW}(\text{lr})$

---

## 163 4 Training

164 This section overviews the datasets and methods used to pre-train MSAMamba.

### 165 4.1 Pre-Training: MultiZ100Way

166 During model pre-training, we leverage the MultiZ100Way dataset, which consists of an MSA of the  
167 length of the human genome without any gap sequences<sup>13</sup> in the human sequence. It also consists  
168 of 99 auxiliary aligned sequences (with gap sequences) from related species. This data has been  
169 curated from the public UCSC Genome Browser [34]. We use a modified version of this dataset,  
170 which excludes ten auxiliary sequences of organisms that are very similar to those of humans [3].  
171 This modification was done to decrease training time and memory requirements while losing minimal  
172 auxiliary information.<sup>14</sup>

173 This dataset was used to train MSA-LM and all MSA-based baseline models<sup>15</sup>. The same random  
174 seeds were also used for data shuffling and batch loading during pre-training for all models.

### 175 4.2 Data Preprocessing

176 The initial training data was collected from the MultiZ100Way dataset by sampling random locations  
177 across the genome and selecting DNA sequences based on the required context length for training  
178 (We use a context length of 1024 across all training steps).<sup>16</sup>

179 Data in the MultiZ100Way dataset was parsed using a tokenizer with a vocabulary size of 6. This  
180 consists of 4 nucleotides, one token for gap sequences, and one mask token. There was no need for  
181 <PAD> tokens due to all excerpts from the dataset being the same length.

182 This data was preprocessed based on the masked language modeling algorithm. This involves masking  
183 15% of the sequence, where 80% of masked tokens are replaced with the <MASK> token, 10% is  
184 replaced with a random token, and the final 10% is not replaced [13].

185 *Note: Only the top sequence in the MSA (the human sequence) is masked due to the focus on the*  
186 *human genome, with other genomes being additional information*

### 187 4.3 Model Sizes

188 We trained 4 different MSA-LM models (see Table 1). Two of these models have a model dimension  
189 of 64, while others have a model dimension of 128. In all cases, we leverage an expansion factor of 2  
190 for the SSM process. In addition, all models contain 3 MSA-LM layers except for one model with a  
191 model dimension of 128. Sequence length was gradually increased across model sizes.

---

<sup>13</sup>Gap sequences occur in MSAs when alignment moves around nucleotides to fit the proper evolutionary configuration, leaving placeholders for locations affected by shift/insertion/deletion mutations

<sup>14</sup>The MultiZ90Way is publicly accessible through HuggingFace datasets [29]

<sup>15</sup>Non-MSA models used as baselines were trained on the regular human genome without MSA augmentation

<sup>16</sup>We were unable to train on the entire genome due to lack of computational power

192 All models were trained on the same amount of data. However, only the final model ( $d_{model} = 128$   
 193 and sequence length = 1024) is leveraged for its evaluations due to it having the highest performance  
 194 based on training and validation loss results.

Table 1: Table of model configurations that underwent the training, fine-tuning, and evaluation processes with comparison to baseline models with similar parameters

$d_{model}$	$d_{ssm}$	$n_{layers}$	SEQ. LEN
64	128	3	128
64	128	3	512
128	256	3	1024
128	256	4	1024

#### 195 4.4 Hyperparameter Selection

196 MSA-LM was trained using a masked language modeling formulation<sup>17</sup>. This method involves using  
 197 Cross Entropy Loss on logit outputs to determine the accuracy of mask predictions (see Algorithm 1).  
 198 The Adam optimizer was used for all training runs.

199 Before a full training run, we swept across multiple learning rates for an initial epoch of training<sup>18</sup>.  
 200 The following learning rates were evaluated based on first-epoch performance:  $3e-5$ ,  $9e-5$ ,  $3e-4$ ,  
 201  $1e-3$ ,  $8e-3$ <sup>19</sup>. The learning rate of  $3e-4$  was found to perform the best during pre-training. A  
 202 warmup scheduler is used to gradually increase the learning rate from 0 to  $3e-4$  across 25% of all  
 203 gradient steps in the training run.

204 We train on sequences that are 1024 base pairs in length and use a physical batch size of 4 sequences.  
 205 Due to computational constraints, we accumulate gradients across every 12 batches to increase the  
 206 precision of gradient steps. With this formulation, the model is trained on 49152 base pairs per  
 207 gradient step.

208 All training runs use a gradient clip value of 5.0 and a weight decay of  $1e-3$ . In addition, the Adam  
 209 optimizer uses (0.9, 0.95) as beta values.

## 210 5 Fine-Tuning and Evaluation

211 We provide an overview of the datasets and methods used for fine-tuning the MSA-LM model. In  
 212 addition, we use similar formulations of the datasets for baseline models<sup>20</sup>. (Dataset processing  
 213 information in A)

### 214 5.1 Fine-Tuning Method and Parameters

215 All fine-tuning tasks leveraged a full-parameter fine-tuning methodology. In addition, we padded  
 216 all sequences during the fine-tuning process to a length of 1024. The only exception to this padding  
 217 length is during the OMIM and ClinVar tasks, where we fine-tune two models on a sequence length  
 218 of 1024 and two other models on a sequence length of 512.

219 All fine-tuning jobs leveraged the Adam optimizer and similar hyperparameters. We leveraged a  
 220 learning rate of  $3e-4$ , a weight decay value of  $1e-3$ , and betas of (0.9, 0.95).

221 Each fine-tuning process consisted of 3 epochs, each with 15000 steps. Fine-tuning was done using a  
 222 batch size of 4 and gradient accumulation across every 8 iterations. This amounts to 32768 base pairs  
 223 being attended to per gradient step.

<sup>17</sup>Masked language modeling was chosen over causal language modeling to learn full representations of DNA without restrictions from causal masks or specific decoding methods

<sup>18</sup>This epoch used the same shuffling seed to ensure equal performance

<sup>19</sup>a learning rate of  $8e-3$  was leveraged in Mamba and long-convolution-based models

<sup>20</sup>Datasets are modified to use MSA or single-sequence versions based on the capability of the specified baseline model

TASK NAME	GPN-MSA	MSAMAMBA	MSA-LM
CLINVAR (512)	<b>0.967</b>	0.965	0.965
OMIM (512)	0.130	<b>0.131</b>	0.129
CLINVAR (1024)	0.962	<b>0.978</b>	0.976
OMIM (1024)	0.118	0.139	<b>0.143</b>

Table 2: Evaluation of MSA-LM, GPN-MSA, MSAMamba, HyenaDNA, and DNABERT on variant effect prediction tasks using the AUROC metric for ClinVar and AUPRC for OMIM

TASK NAME	DNABERT	HYENADNA	GPN-MSA	MSAMAMBA	MSA-LM
MOUSE ENHANCERS	66.9	85.1	76.4	82.7	<b>86.8</b>
CODING VS INTERGENOMIC	92.5	91.3	90.3	90.0	<b>92.7</b>
HUMAN VS WORM	93.0	96.6	<b>98.9</b>	98.5	98.6
HUMAN ENHANCERS COHN	74.0	<b>74.2</b>	73.1	72.7	72.8
HUMAN ENHANCERS ENSEMBL	85.7	89.2	89.3	88.8	<b>89.7</b>
HUMAN REGULATORY	88.1	93.8	93.5	94.4	<b>95.1</b>
HUMAN NONTATA PROMOTERS	85.6	96.6	90.9	94.2	<b>97.0</b>
HUMAN OCR ENSEMBL	75.1	80.9	76.8	<b>82.5</b>	81.9

Table 3: Evaluation of MSA-LM, GPN-MSA, MSAMamba, HyenaDNA, and DNABERT on GenomicBenchmarks tasks using top-1 accuracy (%) metric

## 224 6 Results

225 We show evaluation results for fine-tuned versions of MSA-LM on Genomic Benchmarks tasks and  
 226 Long-Context ClinVar and OMIM Tasks<sup>21</sup>. In addition, we evaluate inference and training step times  
 227 for MSA-LM and relevant baseline models.

### 228 6.1 Variant Effect Prediction

229 We evaluate MSA-LM on both the ClinVar and OMIM variant effect prediction tasks. Each variant  
 230 effect prediction task involved two fine-tuning jobs: one with a context length of 512, and another  
 231 with a context length of 1024. Results show that MSA-LM performs similarly to MSAMamba at  
 232 context lengths of 1024 and slightly below average with reference to GPN-MSA regarding smaller  
 233 context lengths.

234 This most likely occurs due to the MSA-LM’s bias towards longer sequences during training. In con-  
 235 trast, GPN-MSA’s full self-attention formulation is more robust at shorter context lengths. However,  
 236 MSA-LM is advantageous in longer context lengths due to its training data being mostly from this  
 237 distribution. The model shows similar performance to MSAMamba, with only minor differences in  
 238 metrics. Overall, MSA-LM can generalize to long sequences for downstream tasks with a higher  
 239 computational efficiency compared to previous methods.

### 240 6.2 Genomic Benchmarks

241 In addition to variant effect prediction tasks, we evaluate MSA-LM and baseline models on Genomic  
 242 Benchmarks tasks. We fine-tune the model on sequences of length 1024, and we also evaluate the  
 243 following baseline models:

- 244 • DNABERT (110 million parameters) - a BERT transformer architecture trained to represent  
 245 DNA sequences
- 246 • HyenaDNA - long convolution-based architecture for DNA processing. The HyenaDNA-tiny  
 247 version was used with a model dimension of 128 and a sequence length of 16k
- 248 • MSA-based models: GPN-MSA - a transformer model that processes DNA MSAs.  
 249 MSAMamba - subquadratic MSA model leveraging Mamba selective scan

<sup>21</sup>maximum sequence length is capped at 1024 base pairs due to computational constraints



250 MSA-LM shows state-of-the-art performance in 3 Genomic Benchmarks tasks. While lacking in  
 251 "OCR Ensembl" and "Enhancers Cohn" tasks, MSA-LM shows the highest performance when fine-  
 252 tuning on regulatory sequences (e.g. promoters, enhancers). This shows that MSA-LM's training  
 253 dataset may have been biased towards these regions during training. It is also possible that convolution  
 254 operators inserted in the architecture can efficiently extract regulatory sequence information and  
 255 influence across long-context inputs.

### 256 6.3 Training Complexity Analysis

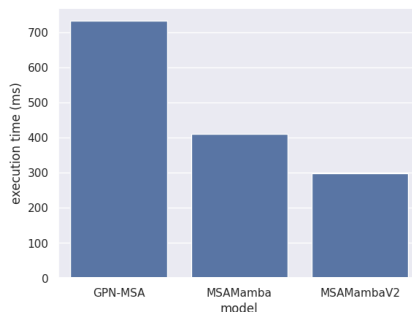


Figure 4: A comparison of time benchmarks for 3 DNA MSA sequence processing models. Each model is evaluated on one NVIDIA T4 GPU to determine the time taken to process the forward and backward pass of a batch of 4 1024-base-pair sequences

257 In addition to experimental evaluations, we provide a wall-clock complexity comparison of MSA-LM.  
 258 Wall clock time-based computational complexity evaluations of MSA-LM, along with 2 baseline  
 259 models (GPN-MSA, MSAMamba) are computed. The time taken to evaluate the forward and  
 260 backward pass of a batch of 4 1024-length sequences is computed<sup>22</sup>. All experiments use a model  
 261 dimension of 128 and default derivations of other model dimensions<sup>23</sup>. We find that MSA-LM has  
 262 the fastest training step performance. This is due to the relative efficiency of the sequence-level mixer  
 263 operation in comparison to MSAMamba and GPN-MSA.

## 264 7 Discussion

265 MSA-LM is a promising architecture for DNA MSA analysis. Previous methods for DNA MSA  
 266 analysis have lacked robust training on long context lengths due to computational complexity con-  
 267 straints. In addition, many previous models were not equipped to extract inductive biases inherent in  
 268 DNA effectively. MSA-LM modifies the previous MSAMamba architecture to fix these problems.  
 269 MSA-LM has higher training efficiency compared to previous methods due to sequence-level pro-  
 270 cessing only happening on the main sequence instead of all sequences. This allows the model to  
 271 be subquadratic in both the sequence and MSA dimension, and remove the restriction of low batch  
 272 sizes due to expensive sequence-level computations. MSA-LM shows state-of-the-art/similar to  
 273 state-of-the-art (SOTA) performance in long-context variant effect prediction tasks. The model also  
 274 shows SOTA performance on Genomic Benchmarks tasks, showing particularly high performance in  
 275 regulatory sequence analysis.

276 MSA-LM can be applied to mutation detection and effect prediction, as well as general causal analysis  
 277 of DNA sequences for editing sequence generation or plasmid generation.

## 278 References

279 [1] Dzmitry Bahdanau, Kyunghyun Cho, and Yoshua Bengio. Neural machine translation by jointly  
 280 learning to align and translate, 2014.

<sup>22</sup>experiment is repeated 20 times per model and averaged for accurate results

<sup>23</sup>e.g.  $d_{attn}$  for GPN-MSA will be  $d_{model}/2$ , Mamba uses a 2x expand on the original  $d_{model}$  value. Others can be found in relevant model repositories

- 281 [2] Bachir Balech, Saverio Vicario, Giacinto Donvito, Alfonso Monaco, Pasquale Notarangelo,  
282 and Graziano Pesole. Msa-pad: Dna multiple sequence alignment framework based on pfam  
283 accessed domain information. *Bioinformatics*, 31(15):2571–2573, March 2015.
- 284 [3] Gonzalo Benegas, Carlos Albors, Alan J. Aw, Chengzhong Ye, and Yun S. Song. Gpn-msa: an  
285 alignment-based dna language model for genome-wide variant effect prediction. October 2023.
- 286 [4] Guy E. Blelloch. Prefix sums and their applications. Technical Report CMU-CS-90-190, School  
287 of Computer Science, Carnegie Mellon University, November 1990.
- 288 [5] T.A. Brown. *Introduction to Genetics: A Molecular Approach*. CRC Press, 2012.
- 289 [6] Tom B. Brown, Benjamin Mann, Nick Ryder, Melanie Subbiah, Jared Kaplan, Prafulla Dhariwal,  
290 Arvind Neelakantan, Pranav Shyam, Girish Sastry, Amanda Askell, Sandhini Agarwal, Ariel  
291 Herbert-Voss, Gretchen Krueger, Tom Henighan, Rewon Child, Aditya Ramesh, Daniel M.  
292 Ziegler, Jeffrey Wu, Clemens Winter, Christopher Hesse, Mark Chen, Eric Sigler, Mateusz  
293 Litwin, Scott Gray, Benjamin Chess, Jack Clark, Christopher Berner, Sam McCandlish, Alec  
294 Radford, Ilya Sutskever, and Dario Amodei. Language models are few-shot learners, 2020.
- 295 [7] Lu Chi, Borui Jiang, and Yadong Mu. Fast fourier convolution. In H. Larochelle, M. Ranzato,  
296 R. Hadsell, M.F. Balcan, and H. Lin, editors, *Advances in Neural Information Processing*  
297 *Systems*, volume 33, pages 4479–4488. Curran Associates, Inc., 2020.
- 298 [8] Rewon Child, Scott Gray, Alec Radford, and Ilya Sutskever. Generating long sequences with  
299 sparse transformers, 2019.
- 300 [9] Kyunghyun Cho, Bart van Merriënboer, Caglar Gulcehre, Dzmitry Bahdanau, Fethi Bougares,  
301 Holger Schwenk, and Yoshua Bengio. Learning phrase representations using rnn encoder-  
302 decoder for statistical machine translation, 2014.
- 303 [10] Hugo Dalla-Torre, Liam Gonzalez, Javier Mendoza Revilla, Nicolas Lopez Carranza, Adam Hen-  
304 ryk Grzywaczewski, Francesco Oteri, Christian Dallago, Evan Trop, Hassan Sirelkhatim,  
305 Guillaume Richard, Marcin Skwark, Karim Beguir, Marie Lopez, and Thomas Pierrot. The  
306 nucleotide transformer: Building and evaluating robust foundation models for human genomics.  
307 *bioRxiv*, 2023.
- 308 [11] Tri Dao, Daniel Y. Fu, Stefano Ermon, Atri Rudra, and Christopher Ré. Flashattention: Fast  
309 and memory-efficient exact attention with io-awareness, 2022.
- 310 [12] Tri Dao and Albert Gu. Transformers are ssms: Generalized models and efficient algorithms  
311 through structured state space duality, 2024.
- 312 [13] Jacob Devlin, Ming-Wei Chang, Kenton Lee, and Kristina Toutanova. Bert: Pre-training of  
313 deep bidirectional transformers for language understanding, 2018.
- 314 [14] Yihe Dong, Jean-Baptiste Cordonnier, and Andreas Loukas. Attention is not all you need:  
315 pure attention loses rank doubly exponentially with depth. In Marina Meila and Tong Zhang,  
316 editors, *Proceedings of the 38th International Conference on Machine Learning*, volume 139 of  
317 *Proceedings of Machine Learning Research*, pages 2793–2803. PMLR, 18–24 Jul 2021.
- 318 [15] Yihe Dong, Jean-Baptiste Cordonnier, and Andreas Loukas. Attention is not all you need: Pure  
319 attention loses rank doubly exponentially with depth, 2023.
- 320 [16] Daniel Y. Fu, Tri Dao, Khaled K. Saab, Armin W. Thomas, Atri Rudra, and Christopher Ré.  
321 Hungry hungry hippos: Towards language modeling with state space models, 2023.
- 322 [17] Daniel Y. Fu, Elliot L. Epstein, Eric Nguyen, Armin W. Thomas, Michael Zhang, Tri Dao, Atri  
323 Rudra, and Christopher Ré. Simple hardware-efficient long convolutions for sequence modeling,  
324 2023.
- 325 [18] Katarína Grešová, Vlastimil Martinek, David Čechák, Petr Šimeček, and Panagiotis Alexiou.  
326 Genomic benchmarks: a collection of datasets for genomic sequence classification. *BMC*  
327 *Genomic Data*, 24(1):25, 2023.

- 328 [19] Albert Gu and Tri Dao. Mamba: Linear-time sequence modeling with selective state spaces,  
329 2023.
- 330 [20] Albert Gu, Tri Dao, Stefano Ermon, Atri Rudra, and Christopher Re. Hippo: Recurrent memory  
331 with optimal polynomial projections, 2020.
- 332 [21] Albert Gu, Karan Goel, and Christopher Ré. Efficiently modeling long sequences with structured  
333 state spaces, 2022.
- 334 [22] A. Hamosh. Online mendelian inheritance in man (omim), a knowledgebase of human genes  
335 and genetic disorders. *Nucleic Acids Research*, 33(Database issue):D514–D517, December  
336 2004.
- 337 [23] Kaiming He, Xiangyu Zhang, Shaoqing Ren, and Jian Sun. Deep residual learning for image  
338 recognition, 2015.
- 339 [24] Sepp Hochreiter and Jürgen Schmidhuber. Long short-term memory. *Neural computation*,  
340 9(8):1735–1780, 1997.
- 341 [25] Sukjun Hwang, Aakash Lahoti, Tri Dao, and Albert Gu. Hydra: Bidirectional state space  
342 models through generalized matrix mixers, 2024.
- 343 [26] M I Jordan. Serial order: a parallel distributed processing approach. technical report, june  
344 1985-march 1986. 5 1986.
- 345 [27] Feyza Duman Keles, Pruthuvi Mahesakya Wijewardena, and Chinmay Hegde. On the computa-  
346 tional complexity of self-attention, 2022.
- 347 [28] Melissa J. Landrum, Jennifer M. Lee, George R. Riley, Wonhee Jang, Wendy S. Rubinstein,  
348 Deanna M. Church, and Donna R. Maglott. Clinvar: public archive of relationships among  
349 sequence variation and human phenotype. *Nucleic Acids Research*, 42(D1):D980–D985, Novem-  
350 ber 2013.
- 351 [29] Quentin Lhoest, Albert Villanova del Moral, Yacine Jernite, Abhishek Thakur, Patrick von  
352 Platen, Suraj Patil, Julien Chaumond, Mariama Drame, Julien Plu, Lewis Tunstall, Joe Davison,  
353 Mario Šaško, Gunjan Chhablani, Bhavitvya Malik, Simon Brandeis, Teven Le Scao, Victor  
354 Sanh, Canwen Xu, Nicolas Patry, Angelina McMillan-Major, Philipp Schmid, Sylvain Gugger,  
355 Clément Delangue, Théo Matussière, Lysandre Debut, Stas Bekman, Pierric Cistac, Thibault  
356 Goehringer, Victor Mustar, François Lagunas, Alexander M. Rush, and Thomas Wolf. Datasets:  
357 A community library for natural language processing, 2021.
- 358 [30] Zeming Lin, Halil Akin, Roshan Rao, Brian Hie, Zhongkai Zhu, Wenting Lu, Nikita Smetanin,  
359 Robert Verkuil, Ori Kabeli, Yaniv Shmueli, Allan dos Santos Costa, Maryam Fazel-Zarandi,  
360 Tom Sercu, Salvatore Candido, and Alexander Rives. Evolutionary-scale prediction of atomic  
361 level protein structure with a language model. July 2022.
- 362 [31] Nelson F. Liu, Kevin Lin, John Hewitt, Ashwin Paranjape, Michele Bevilacqua, Fabio Petroni,  
363 and Percy Liang. Lost in the middle: How language models use long contexts, 2023.
- 364 [32] Inês Lopes, Gulam Altab, Priyanka Raina, and João Pedro de Magalhães. Gene size matters:  
365 An analysis of gene length in the human genome. *Frontiers in Genetics*, 12, February 2021.
- 366 [33] William Merrill, Jackson Petty, and Ashish Sabharwal. The illusion of state in state-space  
367 models, 2024.
- 368 [34] Luis R Nassar, Galt P Barber, Anna Benet-Pagès, Jonathan Casper, Hiram Clawson, Mark  
369 Diekhans, Clay Fischer, Jairo Navarro Gonzalez, Angie S Hinrichs, Brian T Lee, Christopher M  
370 Lee, Pranav Muthuraman, Beagan Nguy, Tiana Pereira, Parisa Nejad, Gerardo Perez, Brian J  
371 Raney, Daniel Schmelter, Matthew L Speir, Brittney D Wick, Ann S Zweig, David Haussler,  
372 Robert M Kuhn, Maximilian Haeussler, and W James Kent. The ucsc genome browser database:  
373 2023 update. *Nucleic Acids Research*, 51(D1):D1188–D1195, November 2022.

- 374 [35] Eric Nguyen, Michael Poli, Matthew G Durrant, Armin W Thomas, Brian Kang, Jeremy  
375 Sullivan, Madelena Y Ng, Ashley Lewis, Aman Patel, Aaron Lou, Stefano Ermon, Stephen A  
376 Baccus, Tina Hernandez-Boussard, Christopher Re, Patrick D Hsu, and Brian L Hie. Sequence  
377 modeling and design from molecular to genome scale with evo. February 2024.
- 378 [36] Eric Nguyen, Michael Poli, Marjan Faizi, Armin Thomas, Callum Birch-Sykes, Michael  
379 Wornow, Aman Patel, Clayton Rabideau, Stefano Massaroli, Yoshua Bengio, Stefano Ermon,  
380 Stephen A. Baccus, and Chris Ré. Hyenadna: Long-range genomic sequence modeling at single  
381 nucleotide resolution. 2023.
- 382 [37] Georgia Pechlivanidou and Nicholas Karampetakis. Zero-order hold discretization of general  
383 state space systems with input delay. *IMA Journal of Mathematical Control and Information*,  
384 39(2):708–730, April 2022.
- 385 [38] Michael Poli, Stefano Massaroli, Eric Nguyen, Daniel Y. Fu, Tri Dao, Stephen Baccus, Yoshua  
386 Bengio, Stefano Ermon, and Christopher Ré. Hyena hierarchy: Towards larger convolutional  
387 language models, 2023.
- 388 [39] Yanay Rosen, Yusuf Roohani, Ayush Agarwal, Leon Samotorčan, Stephen R. Quake, and Jure  
389 Leskovec. Universal cell embeddings: A foundation model for cell biology. November 2023.
- 390 [40] Melissa Sanabria, Jonas Hirsch, Pierre M. Joubert, and Anna R. Poetsch. Dna language model  
391 grover learns sequence context in the human genome. *Nature Machine Intelligence*, July 2024.
- 392 [41] Yair Schiff, Chia-Hsiang Kao, Aaron Gokaslan, Tri Dao, Albert Gu, and Volodymyr Kuleshov.  
393 Caduceus: Bi-directional equivariant long-range dna sequence modeling, 2024.
- 394 [42] Mohammad Yaseen Sofi, Afshana Shafi, and Khalid Z. Masoodi. Chapter 6 - multiple se-  
395 quence alignment. In Mohammad Yaseen Sofi, Afshana Shafi, and Khalid Z. Masoodi, editors,  
396 *Bioinformatics for Everyone*, pages 47–53. Academic Press, 2022.
- 397 [43] Vishrut Thoutam and Dina Ellsworth. MSAMamba: Adapting subquadratic models to long-  
398 context DNA MSA analysis. In *ICML 2024 Workshop on Theoretical Foundations of Foundation*  
399 *Models*, 2024.
- 400 [44] Ashish Vaswani, Noam Shazeer, Niki Parmar, Jakob Uszkoreit, Llion Jones, Aidan N Gomez,  
401 Łukasz Kaiser, and Illia Polosukhin. Attention is all you need. In I. Guyon, U. Von Luxburg,  
402 S. Bengio, H. Wallach, R. Fergus, S. Vishwanathan, and R. Garnett, editors, *Advances in Neural*  
403 *Information Processing Systems*, volume 30. Curran Associates, Inc., 2017.
- 404 [45] Biao Zhang and Rico Sennrich. Root mean square layer normalization, 2019.

## 405 A Fine-Tuning Datasets

### 406 A.0.1 Variant Effect Prediction Tasks

407 We use the OMIM and ClinVar Datasets during the evaluation process. The OMIM dataset relates  
408 gene sequences to different genetic disorders and their forms [22], while ClinVar relates aggregated  
409 gene variance information to overall human health [28]. Fine-tuning on this dataset evaluates a DNA  
410 MSA model’s ability to perceive overall and individual gene relationships to determine its properties.  
411 The addition of MSA information provides key evolutionary information that is useful for these tasks  
412 [3].

413 These two datasets were used at two sequence lengths: 512, and 1024. MSA-LM is trained on  
414 sequence lengths of 1024, while previous models were trained with sequence lengths varying from  
415 128 base pairs to 16 kilo-base pairs depending on model capabilities. We compare evaluations from  
416 the fine-tuning processes across these two context windows as a median context window for all  
417 models to generalize to.

418 The original OMIM and ClinVar datasets consisted of 128-length sequences. We modified these  
419 original sequences to include the area around the original sequence to add up to larger context lengths.

420 This tests models' abilities to detect and analyze specific mutations and segments within longer  
421 sequences.

422 All sequences were retrieved from the MultiZ90Way database given each sequence's chromosome  
423 index, start indices, and end indices. These sequences were not masked but passed as a tuple with a  
424 binary label as the fine-tuning target.

#### 425 **A.0.2 Genomic Benchmark Tasks**

426 MSA-LM and other relevant models were also evaluated on the GenomicBenchmarks dataset [18].  
427 This dataset consists of 8 different tasks relating to sequence-level classification<sup>24</sup>. The original  
428 GenomicBenchmarks datasets are single-sequence, containing only the human genome. However,  
429 we use start indices, stop indices, and chromosome metadata from the datasets along with the  
430 MultiZ90Way database to generate MSA versions of these evaluation datasets.

431 These datasets were not modified for different sequence lengths and were only trained on their original  
432 sequence lengths.

433 *Note: Ethical considerations were carefully addressed during the data curation/processing step. All*  
434 *genome data used in this study were obtained and modified from publicly available datasets (e.g.,*  
435 *MultiZ100Way, OMIM, ClinVar)*

---

<sup>24</sup>We exclude the first three tasks seen in Table 6.2 from discussion, due to their relatively small size and designation as "demo" or "dummy" datasets